Demand Response Dynamic Modelling of Load Shifting Flexibility under Limited Consumer Observability

José Diogo R. U. S. Peres, Instituto Superior Técnico, Universidade de Lisboa, Lisboa

***Abstract*—Demand flexibility and its responsiveness under price-based control is a major research field. Much attention has being payed to model demand elasticity. However, demand flexibility comes mostly as load shifting, and shifting dynamics have been neglected when modelling demand response. In this study load shifting dynamics are modelled to simulate aggregate responses and analyse their predictability under time-varying prices. A particle hopping cellular automaton model is used to study demand response as a means to perform supply following. With that model, simulation is used to analyse load-shifting main dynamics under indirect control strategies. An analysis was made on how does demand respond to price signals and what implications dynamics may have on predictability and controllability. Also, several properties and limitations of load-shifting w.r.t. target aggregate load or original load density distribution, were analysed.**

***Index Terms*—Demand-Side management, demand response, load shifting, load-following, supply-following, supply dynamics, indirect control.**

I. Introduction

EUROPEAN Commission has recently established frameworks to reach targets for clean energy transition by 2030 and to reach climate neutrality by 2050 [1]. Reaching this targets requires novel solutions.

An impressive body of research has recently been made available in the topic of demand response. Many of the studies focus on specific applications as electric vehicles, water heaters and air-conditioners (HVAC). Plug-in hybrid electric vehicles have been studied has a means to regulate power in form of primary, secondary and tertiary frequency control and other ancillary services [2]. In [3] it is assumed that large groups of electrical loads can be controlled as a single entity to reduce their aggregate power demand and then, focuses on the dynamics of thermostatically controlled loads, modelling them in a way simple enough to be used in control design. With a similar objective, in [4], the dynamics of aggregate thermostatic loads are studied using a partial differential equation model aiming at designing nonlinear load control algorithms.

The current electric grid has a relatively simple architecture, where generation is largely predictable and deliberately dispatched. Demand is also well understood, predictable and passive. However, as penetration of renewable generation increases, together with the also increasing adoption of electric vehicles, this premise is changing at an impressive rate. Renewable Energies introduces variability in generation and with the increasing electrification of heat and transport, demand is predicted to increase considerably whilst becoming less predictable. This changes will contribute to bring challenges on peak-power supply and on what the reliability of electricity infrastructure is concerned. For this matter demand side management assumes a great importance.

Load commitment timescale varies from years or months ahead to real time commitment and, therefore, demand response strategies should be developed in accordance. In what years/months ahead load commitment is concerned much has been studied and time-of-use prices exist for a long time as a way of decreasing peak power demand. Conversely, day of dispatch/use or real time demand side management is a relatively recent subject, but with a lot of attention being given to it nowadays and already being implemented, particularly in the form of reserves or balancing markets. However, in a day ahead load commitment timescale, demand response could assume an important role on what could be called the change of paradigm from a "load following" to a "supply following" paradigm, as suggested in [5].

In the conventional supply-following paradigm generation is being dispatched to follow the current load and is seen as an ancillary service to pick up load ramp between scheduling steps and maintaining the frequency of electricity within the required tolerance. With this changes taking place, the future will see demand being called on to follow supply. For this demand response programs, more flexible demand, relying upon some form of energy storage, is going to assume a key role.

Loads that comply with sufficient elasticity requirement are so diverse that it will force utilities and other entities to deal with the future demand-side resource as a composite of different resource types, whose response characteristics they will have to segment into different classes in order to be able to predict individual class responses. This creates the need for studying demand response main dynamics and their implications on load predictability and control, focusing mainly on its implementation.

II. Load Shifting Dynamics

A. Model for Load Shifting

This study is drawn on top of the model first suggested in [6] and that served, also, as the basis for the study in [7].

Shiftable loads are referred to as interruptible, a subclass of curtailable loads that are perfectly elastic in time, as they rely upon perfect storage, but whose elasticity is confined to a

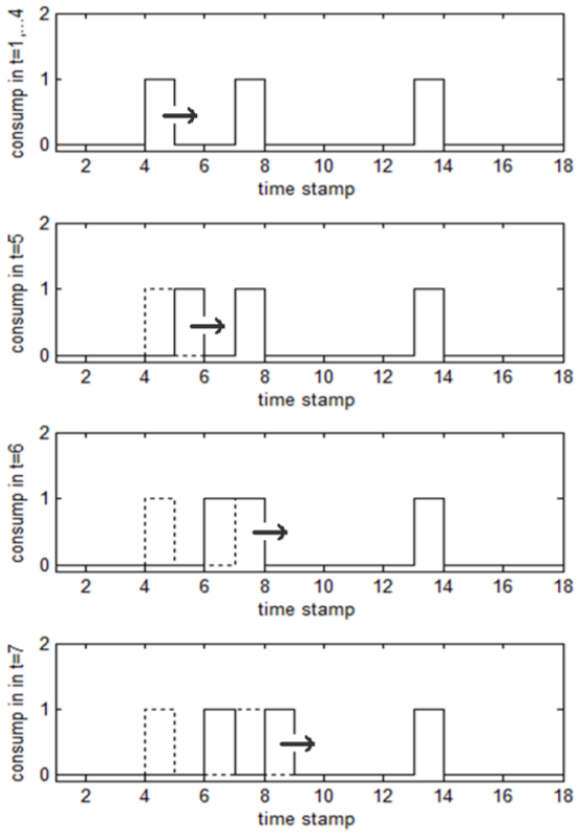

Fig. 1. Illustration of the time-constrained maximum flexibility of a time-shiftable incompressible load from a single user with $\tau = 1$, under the assumptions of instantaneous load use.

time window limited ahead by a given time for load use. An example of such a load is an electric water heater whose time to heat the water is initially scheduled to a period, say $[s, s+\tau]$, that ends a few periods before the time instant u required to use the hot water, i.e., $u > s + \tau$. The load "particle" that corresponds to the power consumption used during the storage period (for water heating) can be shifted ahead in time until $t = u - \tau$ without anticipated discomfort.

In this thesis, the time window is set to its theoretical maximum assuming that (i) the load use is instantaneous and (ii) the original scheduling of storage is set to start immediately after every such use, anticipating the original storage period $[s, s + \tau]$ as much as possible and this way maximizing the room for shifting it ahead in time. Under such assumptions, the original load particles are flexible to be moved ahead as long as they do not overlap the scheduled times of use, u.

Fig. 1 illustrates the dynamics of load-shifting for a single user under the assumptions stated above. The figure shows four plots in consecutive time instances. In the upper plot, the original schedule of load particles is shown. The schedule can be changed at $t = 4$ by shifting the first particle ahead in time. The lower plots show the successive shifting of load particles: in the second and third plots the schedule at $t = 5$ and $t = 6$ is obtained after shifting the first particle once and again; in the fourth plot, the first particle could no longer be shifted

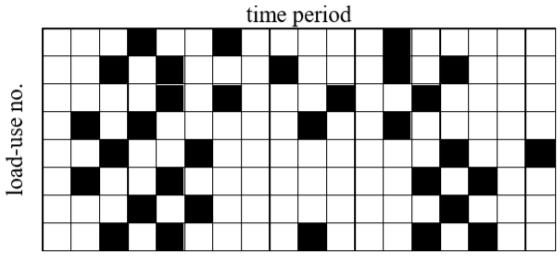

Fig. 2. Two-dimensional lattice of cells representing the original schedule of load uses for a population of uses at $k = 0$ whose flexibility will be explored in $k > 0$ (not illustrated here)

as there was another particle ahead, so, the second particle is moved ahead instead.

For simplicity of notation, it is assumed throughout the study that $\tau = 1$ and use indifferently periods, k, and time stamps, t.

B. Algorithm for Indirect Control

Particle hopping models have been used to simulate a variety of dynamic processes, including traffic-flow [8], [9]. Recently particle hopping models were used to simulate load shifting dynamics [6], [7], for direct control. In those models, each load shifting process is simulated as a particle hopping process in a one-dimensional lattice of cells (a string of cells), each cell representing a time period, k. In the lattice, cells are either occupied by exactly one load particle or are empty, and shifting takes place by hopping between cells in one direction only (the time direction). Because particles can only be shifted ahead onto empty cells, the process of consecutive shifting can be seen as a travelling process with elastic collisions with particles ahead. See Fig. 1 to notice that there is a collision in $k = 6$.

The *population* of load-uses was then modelled as a two-dimensional lattice of cells, one being the time-period dimension of the schedule and the other being the user-number dimension. Fig. 2 illustrates one such lattice for height uses and heighten time periods. Note that the schedule depicted in the first row of the lattice (first user) corresponds to Fig. 1's original schedule.

In [6], the shifting dynamics for ideal direct control over hidden shifting constraints, were analysed, as enabled by future ICT and imposed by the confidentiality of user load schedules, respectively. In [7], the behavior of the model under indirect control, was analysed. The analysis relied on a simple Cellular Automaton (CA) algorithm that simulated real-time control over the aggregate output of a population of shiftable loads. The following definitions help in understanding the proposed algorithm design:

$$p(k) = \sum_{n=1}^{N} d_n(k), \quad k = 1, ..., T \tag{1}$$

$$d_n(k) \in \{0, 1\} \quad n = 1, ..., N; \quad k = 1, ..., T \tag{2}$$

where d_n is the load demand of user n.

A possibility to incentivize users to postpone their consumption would be to, actually, broadcast a price incentive to be paid to users, $\pi(k)$, for every time there is a response to a shifting call. In this case let us suppose each user bids a price π_n to be rewarded for shifting load use n.

Let us define the target output of the aggregate load in time period k by $p^*(k)$. For this experience, based on the model described, a simple algorithm is proposed. The following algorithm summarizes the main steps of the cellular automaton indirect control algorithm implemented:

$Set\ k = 0\ ;\ n = 0\ ;$
for $k = 1, ..., T$ **do**
  if $\pi_n > \pi^*(k)$ **then**
    if $d_n(k) = 1\ \Lambda\ d_n(k+1) = 0$ **then**
      $Make\ d_n(k) = 0;\ d_n(k+1) = 1;$
      $Update\ p(k)\ with\ (1);$
    else
      $Break;$
    $Store\ p(k);$

Fig. 3 illustrates the output $p(k)$ obtained with a population of $N = 5,000$ uses and the corresponding lattice of user responsive actions for a triangular load-following target function, $p^*(k)$. Results are shown in three different perspectives:

1) Evolution in time of the normalized aggregate output that results from individual load responses, $\hat{p}$;
2) Evolution of the number of responsive actions – population shifting velocity $v(t)$ - necessary to undertake the changes in aggregate output;
3) The positions of such responsive actions in the two-dimensional lattice of cells – to identify responsive user positions, v_n.

C. Model for Price-Velocity Characteristic

In [7] the price evolution $\pi^*(k)$ was combined with the evolution of the number of responses in time to synthesize the information obtained in the learning experience. Like before, the relative number of responses is referred by shifting velocity, v, i.e.:

$$v(k) \equiv \sum_{n=1}^{N} v_n(k),\ v_n \in \{0, 1\}, \quad n = 1, ..., N \tag{3}$$

where $v_n(k)$ defined to be: unitary if a particle n is shifted in time k; and zero, otherwise.

It is important to note that, as shown before, the changes in aggregate load necessary to yield p^* in time k $\delta p^*(k) = p^*(k) - \hat{p}$, are obtained by controlling the population velocity, as

$$\delta p^*(k) = -v(k+1) + v(k) \tag{4}$$

The characteristic built from the learning experience with $N = 5,000$ uses is depicted in Fig. 4 assuming that the users' population bidding function $b(n) : n \to \pi_n$ is linear, i.e., that $\pi_n = \alpha n/N$. The characteristic exhibits hysteresis caused by the supply dynamics introduced by the shifting process.

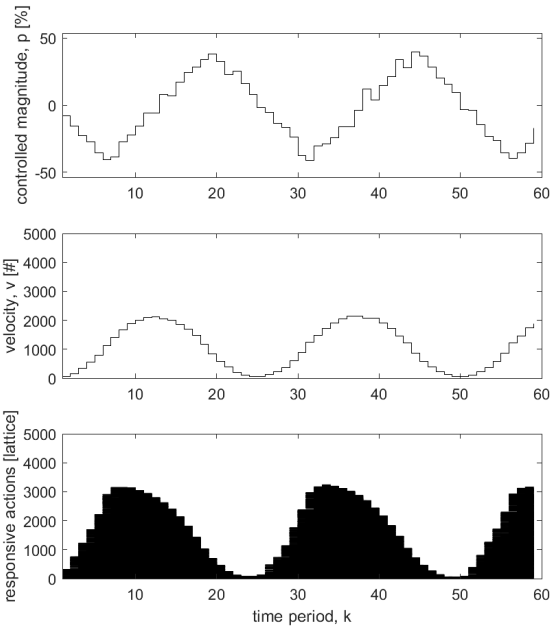

Fig. 3. Load shifting aggregate response from indirect control over a population of $N = 5,000$ uses. The target function is a triangular wave function with magnitude of 40% of the average load. The lattice has an average density of $\hat{d} = 0.167$ load particles per period.

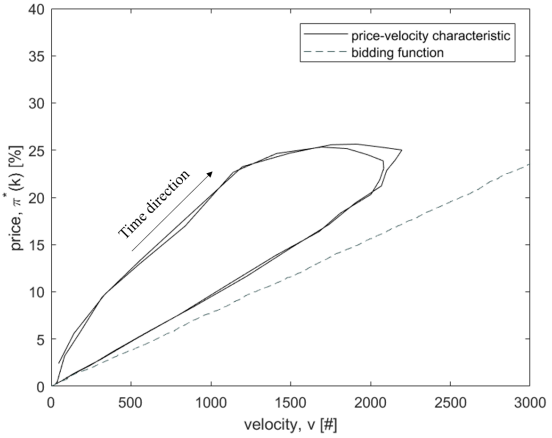

Fig. 4. Price incentive vs. population velocity. Trajectories obtained from experience with $N = 5,000$ uses subject to the indirect price based control process illustrated in Fig. 3 for a linear bidding function with $\alpha = 0.4$.

As it is shown in [7] for large density values the process can be approximated by an ordinary difference equation in time, written as:

$$v^{k+1} \approx \begin{cases} v^k \dfrac{1 - 2\hat{d}}{1 - \hat{d}} + b^{-1}(\pi^k) \cdot \hat{d} & \Leftarrow v^{k+1} > v^k \\ b^{-1}\left(\pi^{k+1}\right)(1 - \hat{d}) & \Leftarrow otherwise \end{cases} \tag{5}$$

The equation can, then, be used to generalize the learning process to other densities and other load target functions. Fig. 6 illustrates the approximate price-response characteristic, as modelled by (5), for different average load densities, $\hat{d}$.

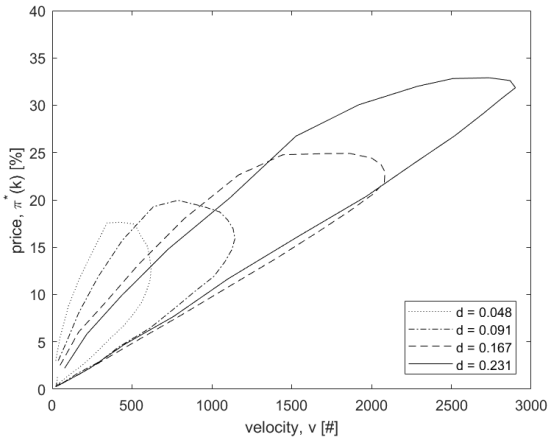

Fig. 5. Price incentive vs. population velocity. Trajectories obtained from experience with different density populations of 5,000 uses subject to the indirect price based control process, with the same triangular target aggregate load function as in Fig. 3, for a linear bidding function with $\alpha = 0.4$

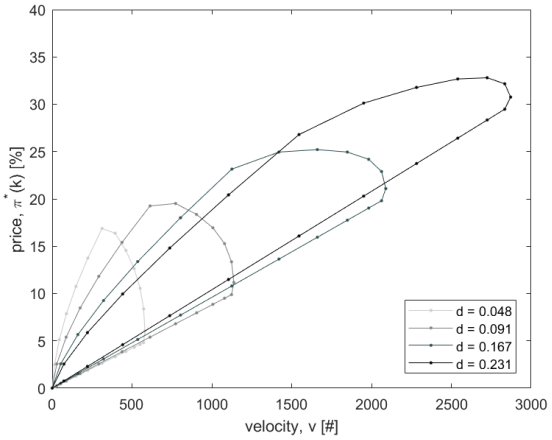

Fig. 6. Price incentive vs. population velocity. Trajectories obtained from experience with different density populations of 5,000 uses subject to the indirect price based control process, with the same triangular target aggregate load function as in Fig. 3, for a linear bidding function with $\alpha = 0.4$

Fig. 6 in comparison to Fig. 5 shows that, (5), despite not being an exact expression to describe the process, could be seen as a reasonable approximation, especially for higher densities. In fact the expression's domain where velocity is decreasing is not linear nor the domain where velocity is increasing and decreasing prices is described by the same expression as for increasing prices.

From a market perspective, indirect control introduces a dynamical effect into the market clearing process: when a consumer shifts a load particle ahead in a period, this same particle will probably become available to be shifted again in the next period for a similar price, this way expanding particles supply in the future period and consequently decreasing clearing prices for the same target variation of the aggregate load.

III. Predictability under Indirect Control

We might be lead to think that learning could be accomplished only with data on bidding and clearing prices (input) and aggregate load response (output) [10]–[14]. However, (5) highlights the fact that predictability cannot be yield without information on population velocity. It makes clear that the relationship between aggregate output changes, Δp^*, and price, π^*, depend on a state-variable - velocity. If one uses (5) together with (4) to express aggregate output changes on price, one may write:

$$\Delta p^k \approx \begin{cases} \dfrac{\hat{d}}{1-\hat{d}} \cdot v^k - \hat{d} \cdot b^{-1}(\pi^{k+1}) & \Leftarrow \Delta p^*(k) < 0 \\ v^k - (1-\hat{d}) \cdot b^{-1}(\pi^{k+1}) & \Leftarrow otherwise \end{cases} \quad (6)$$

which quantifies the role of velocity in price-based demand response, for a given bidding function $b(n)$.

Load uses cannot be assumed homogeneous, so (6) cannot be used directly to predict load changes induced by price. However, (6), could be used to study how the predictability's dependence on velocity varies with the load itself.

A. Density

Load particle density is defined in [6], as the probability of load demand being unitary. Fig. 6 illustrates the dependence the characteristic has on the value of the average density, $\hat{d}$. Note that, despite the maximum price being different in every curve, the bidding function and the target load-aggregate output is the same. This shows the effect that the average density, $\hat{d}$, has on the number of responses requirements and consequently on the price function, $\pi^*(k)$.

As Fig. 6 shows, the maximum velocity increases with density. This, not only has an effect on supply-following accuracy itself, but also on what predictability is concerned. Note that as density decreases, the curve that represents the price-velocity characteristic moves away from the actual bidding function. Not also that (5) becomes less acurate as density decreases and that the process's hysteresis "width", i.e, the slope difference between ramping-up and ramping-down trajectories, increases. This could bring extra difficulties into the predictability and controllability exercise for lower densities. For higher densities, not only our model better describes the process but it also shows that the characteristic is closer to linearity and therefore, controlability would be made easier with limited information on velocity.

B. Magnitude and Frequency

Fig. 7 shows the effect of magnitude changes on price-velocity characteristic and consequently on supply-following accuracy. As expected, the maximum velocity increases with magnitude, and, so does the process's hysteresis "width", i.e, the slope difference between ramping-up and ramping-down trajectories. This could bring extra difficulties into the predictability and controllability exercise, as magnitude increases. Also, note that, as magnitude reaches the value of $m = 0.7$, the price has already peaked at its maximum ($\pi_{max} = 40\%$),

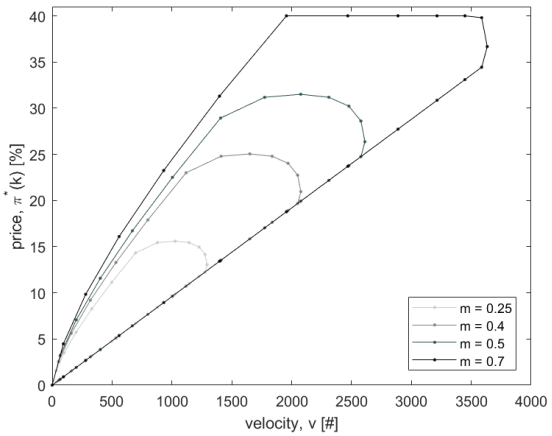

Fig. 7. Price incentive vs. population velocity. Trajectories obtained with (5) for different magnitudes m and constant frequency $f = 0.04$, load density $\hat{d} = 0.16(6)$ and linear bidding function with $\alpha = 0.4$.

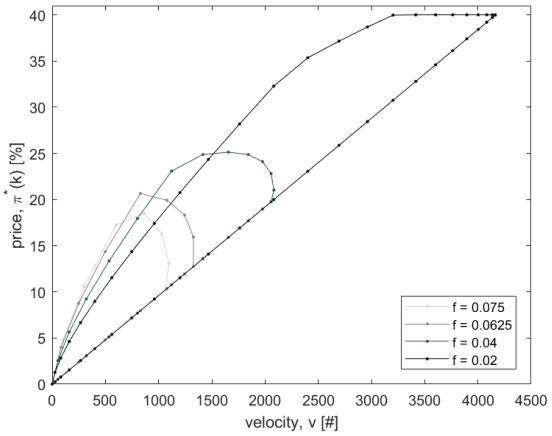

Fig. 8. Price incentive vs. population velocity. Trajectories obtained with (5) for different values of frequency f, a constant magnitude $m = 0.4$, load density $\hat{d} = 0.16(6)$ and linear bidding function with $\alpha = 0.4$.

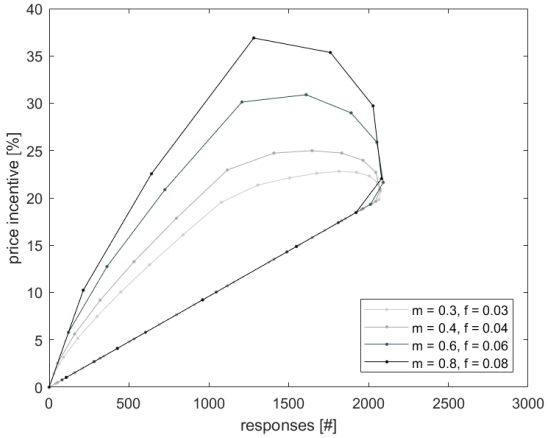

Fig. 9. Price incentive vs. population velocity. Trajectories obtained from experience with 5,000 uses subject to the indirect price based control process, with triangular target aggregate load functions with varying magnitude m and frequency f, keeping a constant m/f relation. Load density is $\hat{d} = 0.16(6)$ and the bidding function is linear with $\alpha = 0.4$

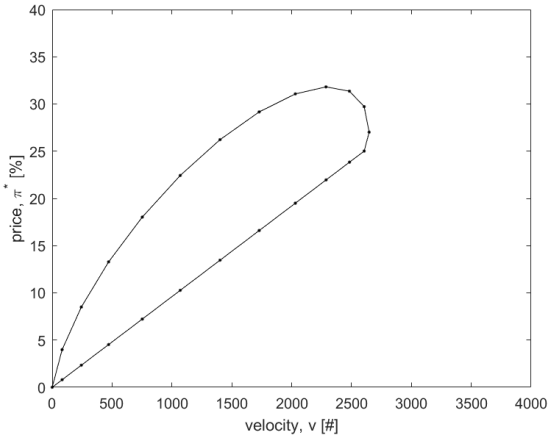

Fig. 10. Price incentive vs. population velocity. Trajectories obtained from experience with 5,000 uses subject to the indirect price based control process, with a sinusoidal target aggregate load function with amplitude of 40% of the average load, for a linear bidding function with $\alpha = 0.4$. The lattice has an average density of $\hat{d} = 0.167$ load particles per period.

meaning that no other users can be called to fulfill the needed number of shifting responses. In this situation, it can be said that supply-following can no longer be accurate.

Despite what one might be led to conclude, frequency changes have the opposite effect of magnitude's. That is because when frequency increases, supply-following becomes less demanding from velocity needs (see Fig. 8). In contrast to magnitude changes' effect on price-velocity, frequency changes do not have a significant impact on hysteresis cycle "width", meaning that predictability would not be affected directly by frequency changes.

Note that, despite not being trivial to guess, in an accurate supply-following process for an aggregate output set to follow a triangle wave function, it is a constant m/f relation that leads to the certainty that supply-following will keep its accuracy, and not a constant slope given by $m \times f$. By looking at Fig. 9, it is evident that maximum velocity is the same for a constant m/f ratio.

Nonetheless, even if a constant m/f leads to a theoretically constant accuracy in supply following, due to the need of predicting the response to a given price function, that might not hold. As it is clear from Fig. 9, when magnitude increases and frequency decreases the cycle's width increases pushing the curve away from linearity and therefore increasing the difficulty in predicting, accurately, the output.

C. Target Load Shape

Fig. 10 depicts the approximate price-velocity characteristic as modelled by (5) for a sinusoidal target function. Since every variable was kept constant except for the target load function shape, both Fig. 5 and Fig. 10 can be compared. From this comparison, it becomes evident that sinusoidal supply-following is more demanding than triangular supply-following. It requires both higher maximum velocity and higher maximum price.

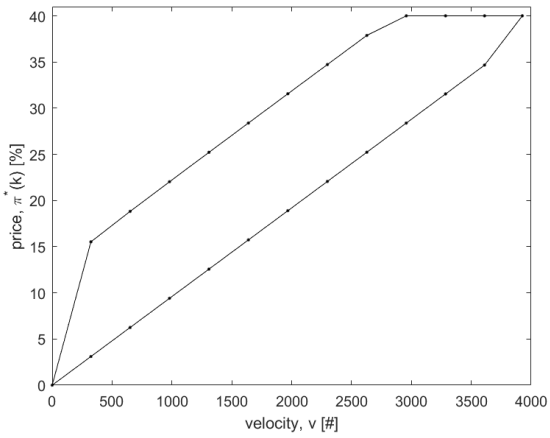

Fig. 11. Price incentive vs. population velocity. Trajectories obtained from experience with 5,000 uses subject to the indirect price based control process, with a square target aggregate load function with amplitude of 40% of the average load, for a linear bidding function with $\alpha = 0.4$. The lattice has an average density of $\hat{d} = 0.167$ load particles per period.

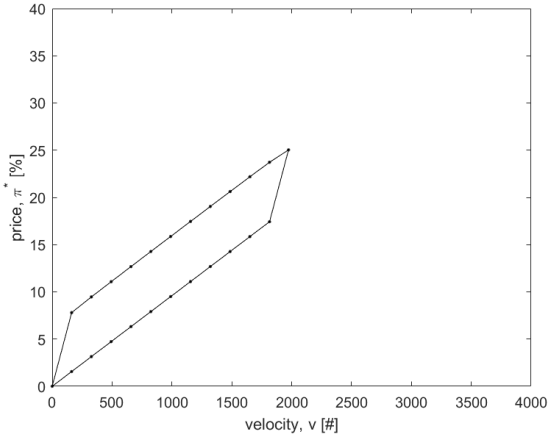

Fig. 12. Price incentive vs. population velocity. Trajectories obtained from experience with 5,000 uses subject to the indirect price based control process, a square target aggregate load function with amplitude of 20% of the average load, for a linear bidding function with $\alpha = 0.4$. The lattice has an average density of $\hat{d} = 0.167$ load particles per period.

Fig. 11 illustrates the approximate price-velocity characteristic again, modelled by (5), this time for a square wave target. From this comparison, it becomes evident that square wave supply-following is more demanding than both the triangular and the sinusoidal functions to a point that, for this magnitude (40%), inaccuracy is not only due to randomness and size effect but also due to the fact that the price reaches its maximum. In this case, to properly compare the price-velocity characteristic with the previous ones, magnitude should be reduced.

Fig. 12 illustrates the the price-velocity characteristic for an experience similar to the one in Fig. 11, except now this time for a square wave target function, $p^*(k)$ with a reduced magnitude of 20%. In this case it becomes clear that the price does not reach its previously defined limit of 40%. However, supply-following is still inaccurate due to randomness and

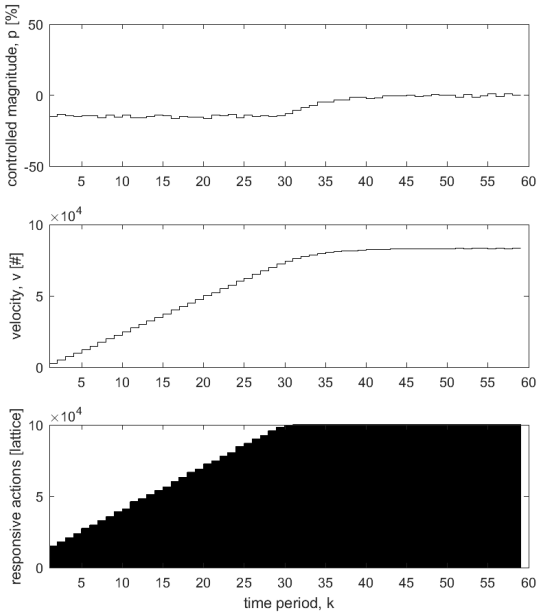

Fig. 13. Load shifting aggregate response from *indirect* control over a population of 50000 uses. The target function is a square wave function with magnitude of 20% of the average load. The lattice has an average density of $\hat{d} = 0.167$ load particles per period.

population size effects that become more visible for the square wave target function.

Note that, as the step duration increases, the more demanding it is to obtain an accurate output function. Contrary to what might be thought, it is more difficult for the load to follow a constant target, different from its average value, than it is for it to ramp-up or ramp-down frequently. This could be explained by the result reached previously, regarding frequency impact on supply-following accuracy. As frequency is reduced, maximum velocity approaches its limit, and therefore the closer supply-following is to become inaccurate.

Fig. 13 shows the output $p(k)$ for an attempt of "smoothing" the original load density to a constant target function with a value 15% higher than the average load. The result is a ramping velocity v. The output function is accurate until velocity reaches its maximum value. At that point the population is unable to keep following the target function $p^*(k)$. It should also be noted that, for this target function, the role of randomness and size assumes is so important that a simulation for a population of $N = 100,000$ had to be carried out to obtain a reasonable accuracy on the target function $p(k)$.

This set of experiences not only shows the effect the target aggregate load function has on the price-velocity characteristic, having a direct influence on the demand for shifting responses, but also illustrates the idea of existence of a maximum velocity above which an accurate output function $p(k)$ is not attainable.

IV. Process Termination

In view of the dynamic characteristic of the process, where velocity assumes such a major part, terminating the control

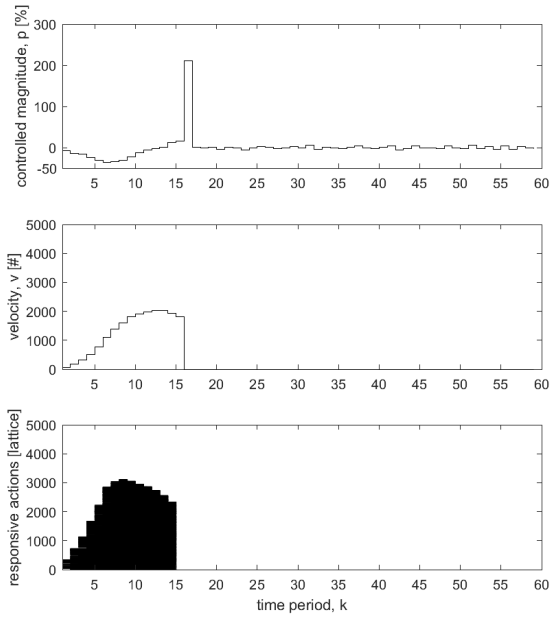

Fig. 14. Load shifting aggregate transient from an interruption (at time period $k = 16$). *Indirect* control over a population of 5000 users. The target function is a triangle wave function with magnitude of 20% of the average load. The lattice has an average density of $\hat{d} = 0.167$ load particles per period.

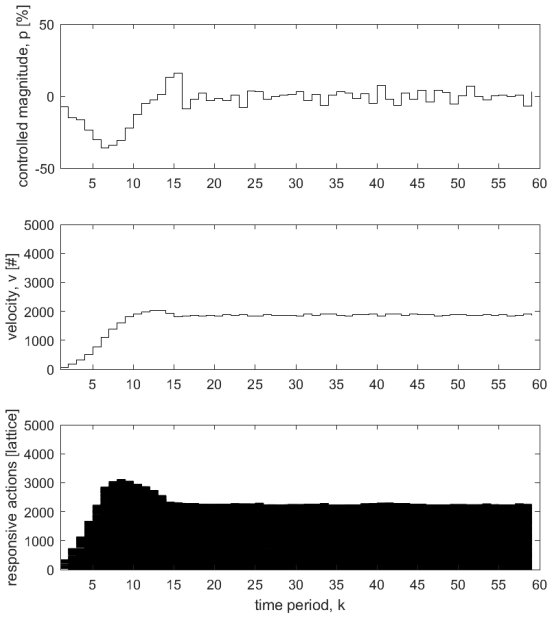

Fig. 15. Load shifting aggregate transient from an interruption. *Indirect* control over a population of 5000 users. The target function is a triangle wave function with magnitude of 20% of the average load. The lattice has an average density of $\hat{d} = 0.167$ load particles per period.

process is not an insignificant matter.

Note that, for an abrupt variation in velocity v, as it represents the integral of the changes in aggregate load Δp, this changes, being its derivative, would tend to be very large. Fig. 14 shows the transient resulting from an abrupt interruption on price incentives and, hence, on velocity. As this figure shows, bringing price incentives to zero, results in a considerable overshoot on load aggregate response, of approximately 200% of the average load, in this case.

Yet, there is a possibility to bring the load aggregate output to its average value without any undesired overshoot. This possibility is to keep the price constant at the value it takes when the process is interrupted. However, this could result in price incentives being paid indefinitely.

An alternative way of terminating the process, bringing load aggregate output to its average value, would be to stop the incentives as velocity crosses zero. At that moment no particle is being shifted and an interruption would not imply any significant transient on controlled magnitude (as seen in Fig. 15).

Once again, from this example, the necessity of having information on velocity data in order to be able to control load-shifting, is reinforced. Without this information, it is not possible to adequately terminate the process.

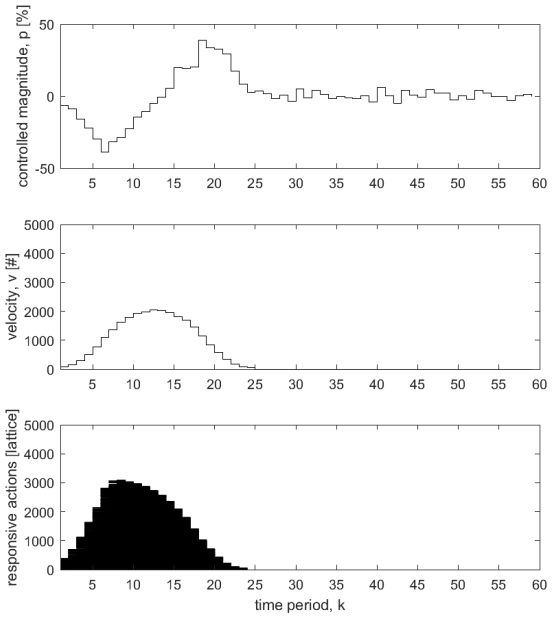

Fig. 16. Load shifting aggregate transient from an interruption. *Indirect* control over a population of 5000 users. The target function is a triangle wave function with magnitude of 20% of the average load. The lattice has an average density of $\hat{d} = 0.167$ load particles per period.

V. Conclusion

In the thesis, individual load-use shifting processes were modelled as a particle hopping process to capture the main dynamics of populations of users under aggregate load profile control. The processes were simulated under indirect control to illustrate the load-following capability of such populations and their dependence on load-use density and population size. The notion of price velocity was introduced and defined as the number of shifting responses projected against price. This price-velocity characteristic is shown to exhibit hysteresis when following periodic load targets. The existence

of hysteresis provides evidence that elasticity alone is not sufficient to model the aggregate response. Aggregate response dynamics and their dependence on prices were then expressed analytically by utilizing velocity to generalize such dependencies. The role of velocity in price-formation was discussed to emphasize that response output cannot be predicted without keeping track of velocity no matter how large the population of users might be. The analytical description of the aggregate response dynamics was, finally, used to study a set of other relevant dependencies and their implications on prediction.

REFERENCES

[1] European Commission, "Going climate-neutral by 2050: A strategic long-term vision for a prosperous, modern, competitive and climate-neutral EU economy," Tech. Rep., 2019.

[2] S. L. Andersson, A. K. Elofsson, M. D. Galus, L. Göransson, S. Karlsson, F. Johnsson, and G. Andersson, "Plug-in hybrid electric vehicles as regulating power providers: Case studies of Sweden and Germany," *Energy Policy*, vol. 38, no. 6, pp. 2751–2762, 6 2010.

[3] C. Perfumo, E. Kofman, J. H. Braslavsky, and J. K. Ward, "Load management: Model-based control of aggregate power for populations of thermostatically controlled loads," *Energy Conversion and Management*, vol. 55, pp. 36–48, 3 2012.

[4] S. Bashash and H. K. Fathy, "Modeling and control of aggregate air conditioning loads for robust renewable power management," *IEEE Transactions on Control Systems Technology*, vol. 21, no. 4, pp. 1318–1327, 2013.

[5] M. Knight, "The Demand Response Paradox," *CGI White Paper Series*, 2016.

[6] P. M. Carvalho and L. A. Ferreira, "Intrinsic limitations of load-shifting response dynamics: Preliminary results from particle hopping models of homogeneous density incompressible loads," *IET Renewable Power Generation*, vol. 13, no. 7, pp. 1190–1196, 2019.

[7] P. M. Carvalho, J. D. Peres, L. A. F. M. Ferreira, M. D. Ilic, and M. Lauer, "Incentive-Based Load Shifting Dynamics and Aggregators Response Predictability," 2020.

[8] K. Nagel and M. Schreckenberg, "A cellular automaton model for freeway traffic," *Journal de Physique I*, vol. 2, no. 12, 1992.

[9] K. Nagel, "Particle hopping models and traffic flow theory," *Physical Review E - Statistical Physics, Plasmas, Fluids, and Related Interdisciplinary Topics*, vol. 53, no. 5, pp. 4655–4672, 9 1996.

[10] N. G. Paterakis, A. Tascikaraoglu, O. Erdinc, A. G. Bakirtzis, and J. P. Catalao, "Assessment of Demand-Response-Driven Load Pattern Elasticity Using a Combined Approach for Smart Households," *IEEE Transactions on Industrial Informatics*, vol. 12, no. 4, pp. 1529–1539, 8 2016.

[11] M. Parvania and M. Fotuhi-Firuzabad, "Demand response scheduling by stochastic SCUC," pp. 89–98, 2010.

[12] N. G. Paterakis, O. Erdinc, A. G. Bakirtzis, and J. P. Catalao, "Load-following reserves procurement considering flexible demand-side resources under high wind power penetration," *IEEE Transactions on Power Systems*, vol. 30, no. 3, pp. 1337–1350, 5 2015.

[13] M. Lauer, "Real-time household energy prediction : approaches and applications for a blockchain-backed smart grid," Ph.D. dissertation, 2019. [Online]. Available: https://dspace.mit.edu/handle/1721.1/121676

[14] M. Lauer, R. Jaddivada, and M. Ilic, "Household Energy Prediction: Methods and Applications for Smarter Grid Design," in *2019 8th Mediterranean Conference on Embedded Computing, MECO 2019 - Proceedings*. Institute of Electrical and Electronics Engineers Inc., 6 2019.